

Experimental study of turret-mounted automatic weapon vibrations

Jiri Balla, Zbynek Krist, and Cong Ich Le

Abstract—The purpose of this article is to introduce a new approach to finding the dynamic characteristics of weapon parts when burst-fired. The result is both vibrations of the parts mounted on track vehicle such as cradle and turret, and the excitation force acting from the weapon onto the mount. The experiments were tested out on a 30 mm soft recoil gas operated cannon turret-mounted on a track vehicle. All results follow from these technical experiments, as well as other derived parameters after frequency and correlation analysis. The outputs can be used for validation of a dynamic model of a weapon system mounted on a track vehicle, and the procedure can be used as an example of a practical technique and methodology for other weapon systems.

Keywords—Correlation function, Density spectrum, Force of shot, Vibration, Weapon system.

I. INTRODUCTION

ANALYSES of mount and carriage vibrations of weapon systems when burst-fired revealed that the cardinal reason defending successful research in this area is not sufficiently based on experimental tests in extreme conditions. Successful management of complex questions regarding measuring in these conditions exceeds the possibilities of a single workplace such as the apparatus and know-how published in measuring methodologies.

Pursuit of achievement of a high hit probability of air targets in course of burst anti-aircraft firing leads to lowering vibrations of the main parts of the tube weapon systems. The main reason is that the other factors influencing fire precision have much lower significance. For example, the surveillance and target acquisition systems enable calculation of bearing and elevation angles with errors of fewer than 2 mrad. The errors of the hull, turret and elevation parts achieve 10 mrad and more due to their vibrations in the vertical plane, see [1], [2]. Then the knowledge of these parts movement when fire-burst is consequential since the correction of aiming in course

of gun fire facilitates an increase in the hit probability. Otherwise, this value falls under 50% for a 500-meter target range. There are three ways of determining weapon system vibrations. One of them is the pure calculation method of the main parts movement. The second technique is a purely experimental investigation of the oscillations of the hull, turret and elevation parts. The last technique is a combination of both previous techniques combined while adding all of the forces acting on the weapon. In [2], [3] dynamic models were published, having eight DOF (degrees of freedom), see Fig. 1, with the structure according to the Fig. 2.

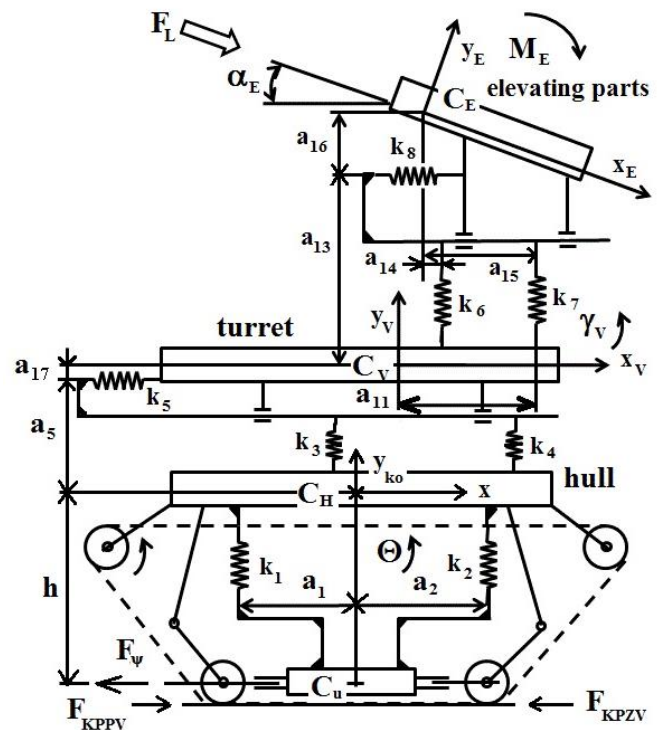


Fig. 1: Dynamic model

The elevating parts consist of an automatic weapon with a recoiling barrel, a breech system, driving springs, other mechanisms, and a cradle, see [4], [5]. The cradle together with the turret is known as the supporting part of the mount. The elevating parts enable the weapon to be aimed in a vertical plane given by the elevation angle α_E . The turret is connected to the hull by means of the azimuth bearing and traversing mechanism.

The coordinates in the dynamic model are labeled as follows:

This work was supported by the research projects: The work presented in this paper has been supported by the research projects of University of Defence, Brno, Czech Republic: Research project of Department of Weapons and Ammunition 2014.).

J. Balla is with the University of Defence, Kounicova 65, 662 10 Brno, Czech Republic (corresponding author to provide phone: +420 973 44 2286; e-mail: jiri.balla@unob.cz) and Alexander Dubček University of Trenčín, Študentská 2, 911 50 Trenčín, Slovakia; email: jiri.balla@tuni.sk.

Z. Krist is with the University of Defence, Kounicova 65, 662 10 Brno, Czech Republic (corresponding author to provide phone: +420 973 44 5011; fax: 00 420 973 44 5011; e-mail: zbynek.krist@unob.cz).

C. I. Le is with the University of Defence, Kounicova 65, 662 10 Brno, Czech Republic; e-mail: ichlecong@gmail.com.

$$[q] = [y_{ko}, \Theta, x_v, y_v, \gamma_v, x_E, y_E, \alpha_E], \quad (1)$$

Where

- y_{ko} – vertical displacement of hull,
- Θ – angular displacement of hull,
- x_v – longitudinal displacement of turret,
- y_v – vertical displacement of turret,
- γ_v – angular displacement of turret,
- x_E – longitudinal displacement of elevating parts,
- y_E – vertical displacement of elevating parts,
- α_E – angular displacement of elevating parts.

All bodies are connected with reduced flexible bindings indicated in Fig. 1 as k_i .

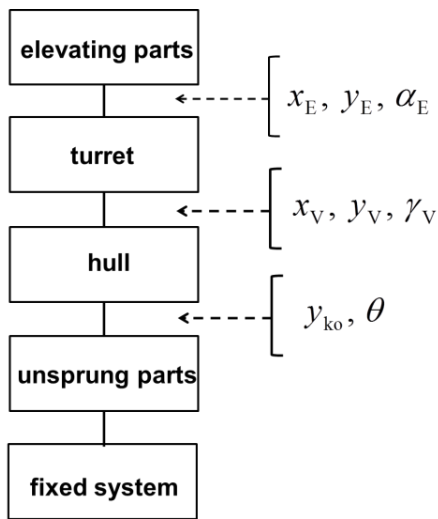


Fig. 2: Weapon structure

Some input characteristics used in this study were set experimentally on a real system. Moreover, behavior of parts such as the cradle and turret during burst-firing was not known beforehand. Their determination using experimental procedures will be described in the following parts.

II. PROBLEM FORMULATION

Fig. 3 shows the location of gauges used for identification of the main parameters for the cradle and turret. The following characteristics were measured on the weapon system:

- linear displacement of recoiling barrel x_z ,
- forces acting onto carriage during burst-fire F_L ,
- vertical acceleration of the board cradle a_{KP} ,
- linear displacements of the front, and rear of turret with respect to the hull y_{VP}, y_{VZ} .

These parameters will be successively discussed in the following chapters. The barrel recoil stroke was determined using a W20 inductance gauge having a ± 20 mm measuring range. The HBM (Hottinger Baldwin Messtechnik, see www.hbm.de), force transducers (strain gauges) located on the weapon casing were electrically connected into the Wheatstone bridge and after laboratory calibration, the forces

acting from the weapon casing onto the board cradle were found. The vertical acceleration a_{KP} of the cradle was measured using a tensometric accelerometer BWH 401 with $5000 \text{ m}\cdot\text{s}^{-2}$ limited acceleration value. Next, the vertical displacements of the turret y_{VP}, y_{VZ} were determined with two W5 inductance gauges, having a $\pm 5 \text{ mm}$ measuring range. As only a simple analog tape recorder was available (with a limited number of channels), two tape recorders were used to record each signal after their amplification, see Fig. 4.

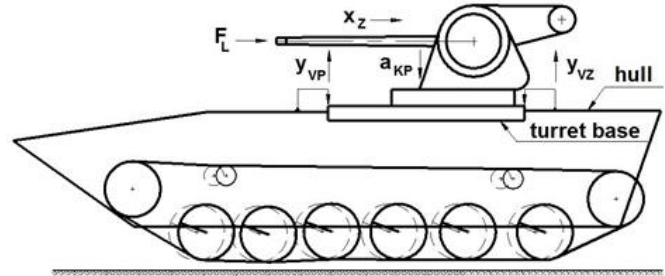


Fig. 3: Gauges location on weapon system

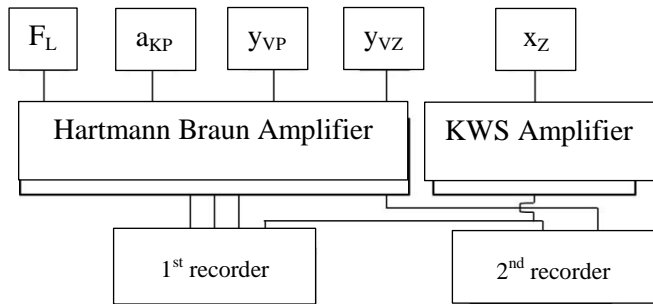


Fig. 4: Measuring chain

From experience, the estimated maximum frequency of the mechanical system was set at 300 Hz, and so a 615 Hz sampling frequency was sufficient for the purpose of signal digitalization. Before digitalization, the signals were filtered by means of 8th order Butterworth low-frequency filters with low-pass filters like: F_L, a_{KP} – 300 Hz, y_{VP}, y_{VZ} – 200 Hz, x_z – 120 Hz.

The raw reported results of the experiments without any corrections are shown in Fig. 5 and Fig. 6. The graphs are shifted in time, and they had to be adjusted to obtain the correct values, mainly for turret motion. This adjustment was done using correlation theory. The recording in the first recorder was moved forward according to the lag time between both recordings - caused by different tape speed and by different start times of the tapes. Every shot is indicated by a minimum value in the barrel recoil graph x_{z_1} , and x_{z_2} .

Fig. 5 shows the recording of the barrel recoil during a six-round burst. Fig. 6 shows the same motion recorded in the second recorder, serving as a synchronizing signal. In addition, the barrel recoil x_{z_2} recording in the second recorder was distorted after the third shot during its registering.

However, the beginning of this registration was clear and corresponded to the first recording of x_{z_1} . The correlation

theory enabled setting of the lag time and to put all signals into time alignment. This solution will be described in the chapter dealing with turret vibration.

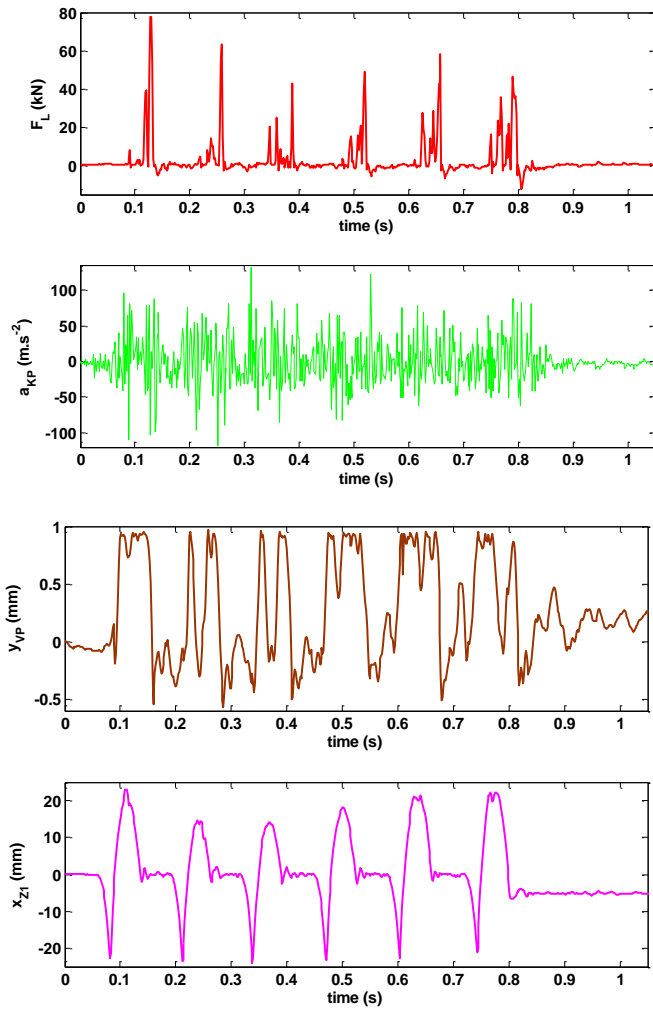


Fig. 5: The first recorder signals

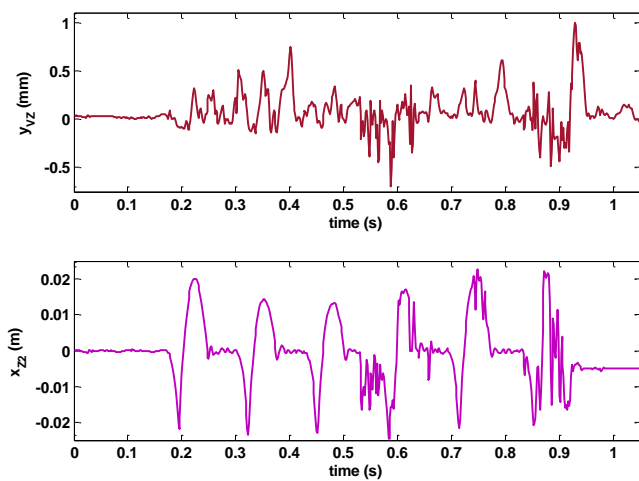


Fig. 6: The second recorder signals

After Next View® software analysis, see [6], the results were exported into Microsoft Excel® format or into ASCII format and finally they were plotted in MATLAB® software. Other options for analyses of the measured data are published

in [7] – [9]. The selected sampling frequency provided a maximum frequency of 307 Hz during determination of the spectrum density using the following formula

$$G_{xx}(f) = \frac{2}{T} \cdot |X_T(jf)|^2, \quad (2)$$

Where

$X_T(jf)$ – Fourier transform of signal,

T – length of signal, f – frequency, j – imaginary unit.

Both, the minimum length of signal T and the minimum frequency in the signal spectrum f_{\min} are connected with equation

$$T \doteq \frac{8}{f_{\min}}. \quad (3)$$

This formula explains the fact that in the course of spectral power density calculations a shift in the lowest frequencies contained in the spectrum signal to higher frequencies can occur.

III. PROBLEM SOLUTION

A. Forces acting onto mount

For automatic weapons held in any type of mount it is necessary to know the forces acting on the different parts of the weapon mount during firing. The effects of shot forces depend on the type of automatic weapon when considering a weapon with gas operated system, recoil system or blowback system, see [10].

Neglecting the inertial and centrifugal forces exerted by the elevation and traversing mechanisms on the mount, the following forces act on the system during firing: the force of shot F_H , the weapon system weight G , the starting torque of barrels group for Gatling type weapons M_{GAT} , see [11], and [12]. When the barrel is fixed relative to the rest of the weapon then all components attaching the weapon to the mount are loaded by the above forces and transmit them to the mount. Weapon weight and starting torque for Gatling guns have small effect compared to the force of shot.

The force of shot is represented by vector acting in the center of gravity of recoiling parts in parallel direction with a barrel axis. Additionally, the dynamic couple $F_H \cdot e$, will be applied to the mount, where e is the distance from recoiling parts center of gravity of recoiling parts to the barrel axis. Usually the dynamic couple can be neglected due to the small value of the distance e .

The variation of the applied force with respect to time depends on the force of shot, its damping and the type of automatic system used. Maximum force of shot is very high (250 kN for 30 mm cannon for example), and therefore the barrels (or the whole weapon with fixed barrel) are designed as recoiling. The force of shot defined in [1], [13] or [14] by the following formula

$$F_H = p_{dh} S - F_{th}, \quad (4)$$

where

p_{dh} is the pressure on the head of the barrel chamber in course of the projectile movement in the barrel.

This force summarizes the forces on the head of the barrel chamber, on the conical part of the barrel chamber and resistances against the projectile motion acting in the opposite direction to the recoil.

The bore area, which depends on the calibre, is:

$$S = \frac{\pi}{4}d^2 \text{ for the smooth bore and } S = \frac{\pi}{4}d^2 + n \cdot a \cdot h \text{ for}$$

the barrel with rifling, where:

d – calibre,

n – number of grooves,

a – width of groove,

h – depth of groove,

p_{dh} – pressure on the chamber head.

The relationship between forces on the projectile and on the bore area corresponding to the calibre in the chamber head is, see [15], [16] or [17]

$$F_{dq} = F_{dh} \frac{m_q}{m_q + \frac{m_w}{2}}, \quad (5)$$

where $F_{dq} = p_{dq}S$ is force on the projectile,

p_{dq} – pressure on the projectile head,

m_q – projectile mass,

m_w – powder charge mass.

The barrel reaction to the resistances against projectile movement is expressed with the following expression

$$F_{th} = fF_t + F_t \tan \alpha, \quad (6)$$

where $F_t = \left(\frac{2i}{d}\right)^2 F_{dq} \tan \alpha$ is total peripheral force,

i – radius of gyration of the projectile,

f – friction coefficient between the projectile and the internal surface of the barrel,

α – rifling angle.

The force of shot is possible to set, see [18] as well, so that this force equals the force on the barrel chamber head with 2% accuracy. Then we can write the calculating formula as

$$F_H = 0.98p_{dh}S. \quad (7)$$

When the projectile exits the barrel, the force of shot can be considered similar to a rocket engine, whose thrust is determined from the following known expression, see [1], [19], [20], and [21],

$$F_H = \frac{dm_w}{dt}w + S(p_u - p_a), \quad (8)$$

where

p_u – pressure at the outlet area (muzzle) of the barrel during after effect time,

p_a – atmospheric pressure,

$\frac{dm_w}{dt}$ – gases mass flow,

w – gases exhaust velocity.

The gases mass flow is possible to determine from the equations published in [1], [2], and [19].

After the projectile has left the barrel muzzle, the force of shot increases as the resistances against projectile movement do not exist and the outflow discharge of the gases from the barrel is equipped with the muzzle brake. This fact is being expressed by the impulse characteristic of a muzzle brake χ , see for example [1], [10], [17], and [18].

One easy way of obtaining the outlet parameters is to use approximation methods - mainly for preliminary design calculations and for weapon systems evaluation. One example is exponential approximation. This method uses the formula, see [1], [22],

$$p_h = p_{hu}e^{\frac{\tau}{b}}, \quad (9)$$

Where

$$b = \frac{\beta - 0.5}{F_{Hu}}v_u m_w - \text{time constant,}$$

v_u – muzzle velocity of the projectile,

F_{Hu} – magnitude of the force of shot when the projectile exits the barrel, and the flow time is

$$\tau = b \ln \frac{p_{hu}}{p_a}.$$

Then the force of the shot in a weapon using a muzzle brake is

$$F_H = \chi Sp.$$

The force of shot of the 30 mm anti-aircraft (AA) cannon used in this study is depicted in Fig. 7.

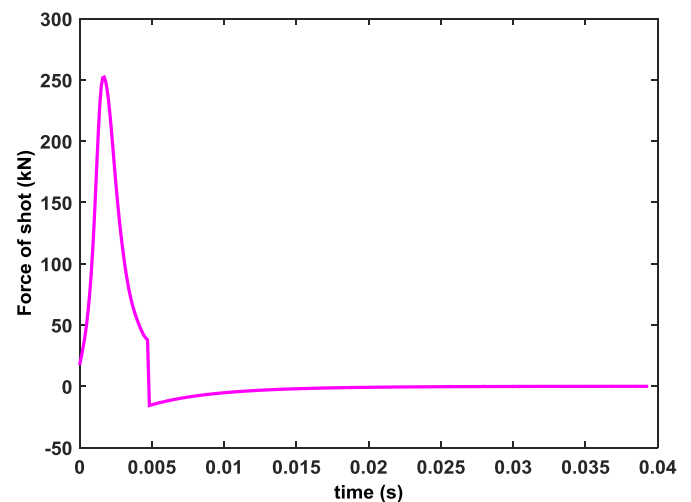


Fig. 7: 30mm AA cannon force of shot

The decrease of force at 0.005 s is given by the muzzle brake with a negative impulse characteristic. It causes braking of recoiling masses at the beginning of the after effect period. The end of the force of shot effect is after 40 milliseconds.

The force of shot impulse I_H is defined according to the equation

$$I_H = \int_0^{t_F} F_H dt. \quad (10)$$

The impulse I_H changes the momentum of the recoiling parts. The mount parts and the hull of the vehicle are loaded, by means of a recoil mechanism or automatic system or shock absorber, using the resultant axial force F_L , while force impulse I_{F_L} is equal to an impulse I_H in duration of one functional cycle.

The impulse of the resultant force is

$$I_{F_L} = \int_0^{t_{FC}} F_{F_L} dt, \quad (11)$$

where

t_{FC} – The time of one functional cycle between two shots.

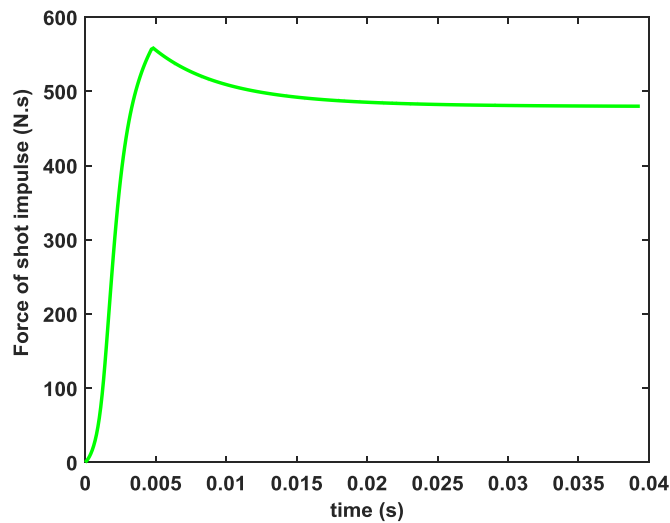


Fig. 8: 30 mm AA cannon force of shot impulse

An accurate knowledge of the total firing impulse I_H is more important than accurate knowledge of the force F_H course and its maximum value $F_{H_{max}}$. This is because most modern weapon mounts are made to be as light as possible and so have a low resonance frequency, in the range 10 – 30 Hz, which is also the frequency of the human body.

In [1], [2], and [10] an explanation was given that maximum movement of the weapon system, and thus the applied stress, is proportional to the impulse I_H , and is minimally affected by the force F_H . When firing a burst, the situation is more complex. However, it can be shown, even for this case, that the load applied to the system is proportional to the average value of the total force loading the mount F_L and not to the maximum value of force F_L and not to the maximum value of force F_H . Impulse of force of shot of a barrel I_H is supposed to be a primary impulse. Time course of a force loading a mount $F_L(t)$ depends not only on a shot impulse, but also on its damping and on the type of automatic system

used. The forces applied to the automatic weapon mount are periodic in nature. The values of the force F_L can be determined by calculation or measurement as it is shown in [3], [23], and [24]. Displacement transducers (for barrel recoil), and strain gauges (for determining the time when the projectile leaves the barrel) were used, see Fig. 9, Fig. 10. The variation in firing force over a six-shot burst is shown in Fig. 5. It can be seen that the force transmitted to the mount had maximum value for the first shot fired. For the second shot there is a reduction in the firing force which is still further reduced for the third shot. It is clear from the analysis that the maximum force applied to the mount occurs at the instant that the barrel is arrested and the breech carrier begins to act on the buffer as shown in Fig. 12, a diagram of a functional weapon, see [10].

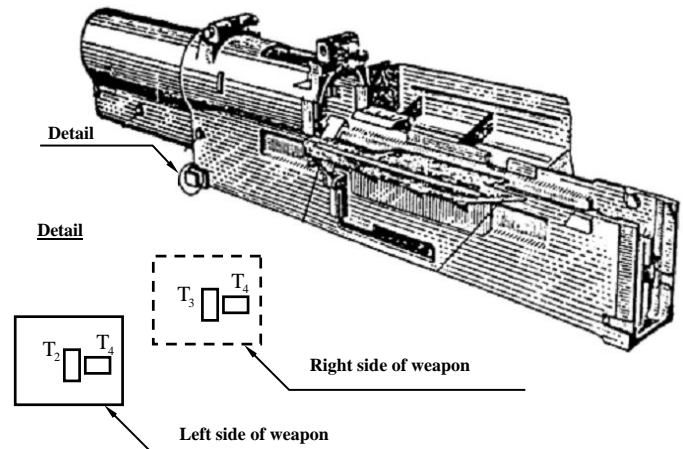


Fig. 9: Position of gauges on 30 mm caliber AA cannon for measuring forces

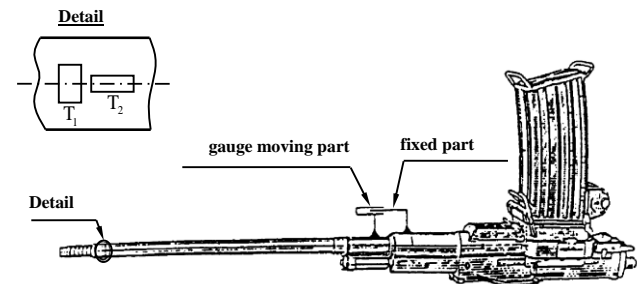


Fig. 10: Position of gauges on 30 mm caliber AA cannon for measuring

A functional diagram helps to explain the weapon operation during one shot. Curve 1 represents barrel recoil, and curve 2 is breech carrier displacement. It is important to note that this system is an example of a soft recoil system, where the barrel is moving forward before shooting. The releasing barrel time is at 100 ms after triggering of the breech carrier from its rear position.

The spectral density variation of the firing force acting on the mount is shown in Fig. 12. This shows that a basic frequency of 7.6 Hz is given by the rate of fire. Frequencies in the range of 15 Hz, 23 Hz and 30 Hz are higher harmonics, and can belong to other weapon parts. For example 23 Hz is contained in the turret vibration.

Comparing two shots in Fig. 5 and Fig. 8, it is clear that the courses of the forces are different mainly from the magnitude point of view. The impulse of the force, acting on the mount and calculated from recordings of the force F_L in Fig. 5, is the same as the impulse of the firing force, which allows quick and simple calculations of the force applied to the mount to be made. In Fig. 13 there is variation in impulses of the force F_L from Fig. 5 applied to the mount of a weapon when firing six-round burst.

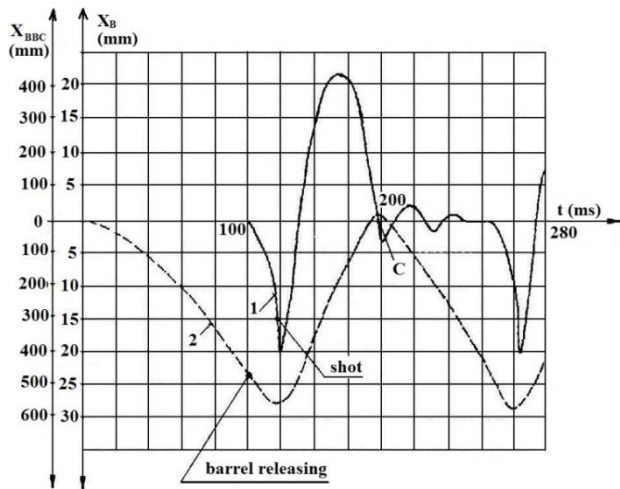


Fig. 11: Functional diagram for 30mm AA cannon

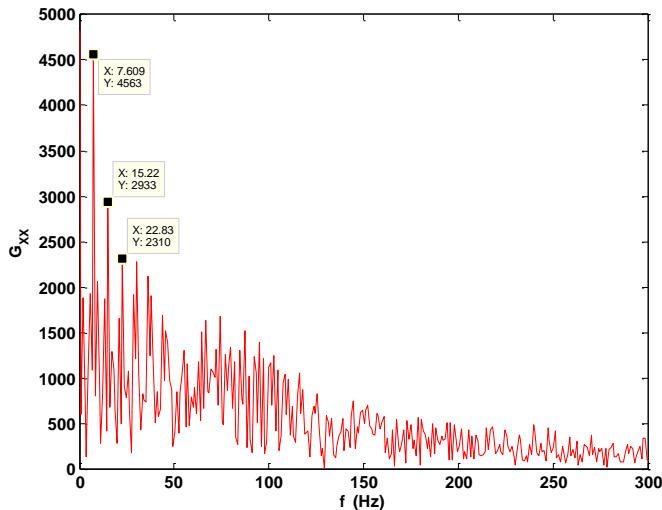


Fig. 12: 30 mm AA cannon spectrum of forces

The weapon is loaded during every shot with the average value of the impulse 485 N·s calculated from six shots. The difference in the impulses between calculations and the experiments is being about 5 % of the force of shot during of one functional cycle, see [24]. It corresponds to presumption that accurate knowledge of the total impulse I_{FL} is more important than an accurate knowledge of the firing force F_L , and its maximum value F_{Lmax} .

This is because most modern weapon mounts and carriages are made to be light as possible.

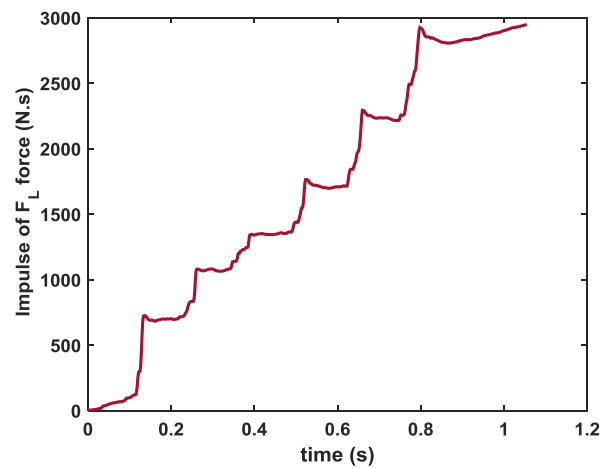


Fig. 13: Impulses of force acting on to mount

B. Cradle vibration

From the time flow of cradle vibration in Fig. 4, it is possible to estimate that it has a wide spectrum and its normalized correlation function is very narrow, see [9], [25], and [26]. Fig. 13 and Fig. 14 confirm these prerequisites. The basic statistical characteristics of cradle acceleration are mean value = $0.51 \text{ m}\cdot\text{s}^{-2}$, minimum value = $-117 \text{ m}\cdot\text{s}^{-2}$, maximum value = $131 \text{ m}\cdot\text{s}^{-2}$, standard deviation = $31 \text{ m}\cdot\text{s}^{-2}$, and median = $-2.29 \text{ m}\cdot\text{s}^{-2}$. High values of acceleration most likely belong to instant values of the acceleration of individual components contained in the signal spectrum.

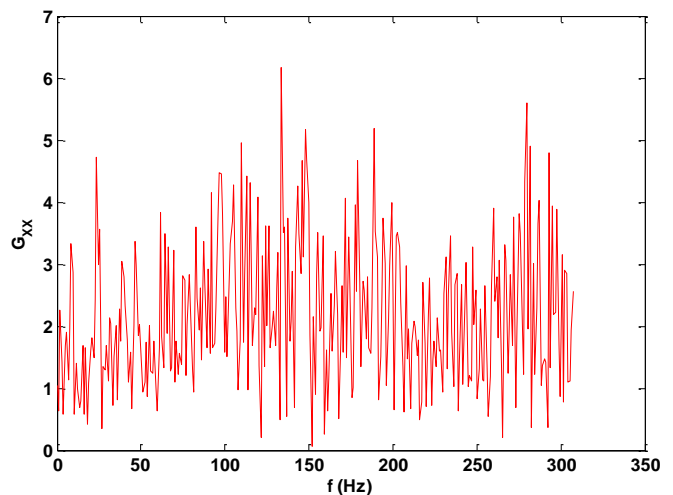


Fig. 14: Spectrum density of cradle acceleration

Other cradle kinematic parameters, which can be determined, are absolute velocity and absolute displacement with respect to the basic system displayed shown in Fig. 16, and Fig. 17. The results were obtained after double integration of the input acceleration displayed in Fig. 5.

It is necessary to note that they are absolute parameters with respect to the Earth. The high values of displacement were caused by vibration due to the turret limited stiffness of the elevation gear, and by hull vibrations that acts as low-pass filter on the whole system, see [2], [3] and [27].

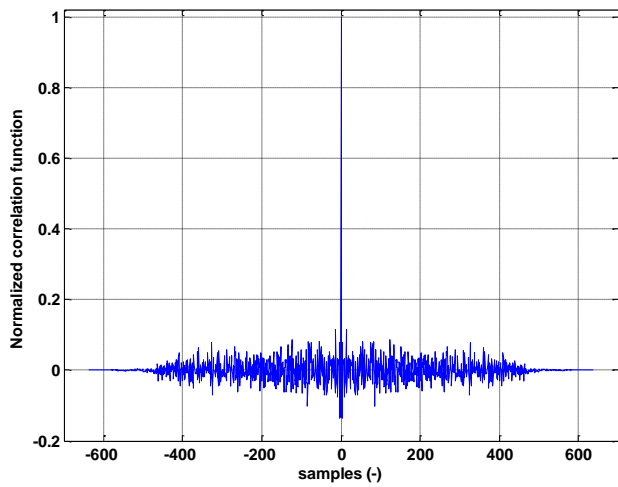


Fig. 15: Correlation function of cradle acceleration

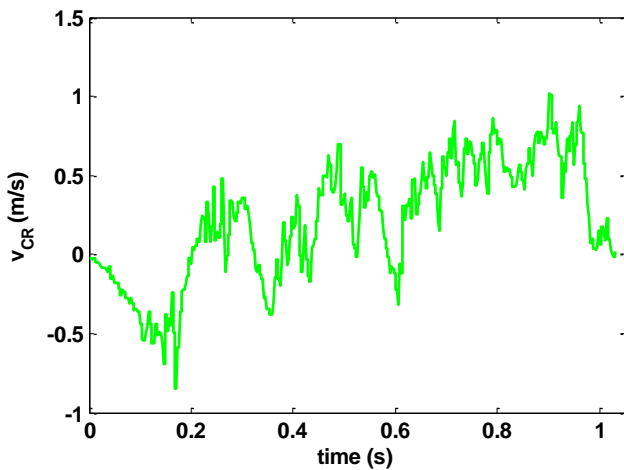


Fig. 16: Cradle vertical velocity

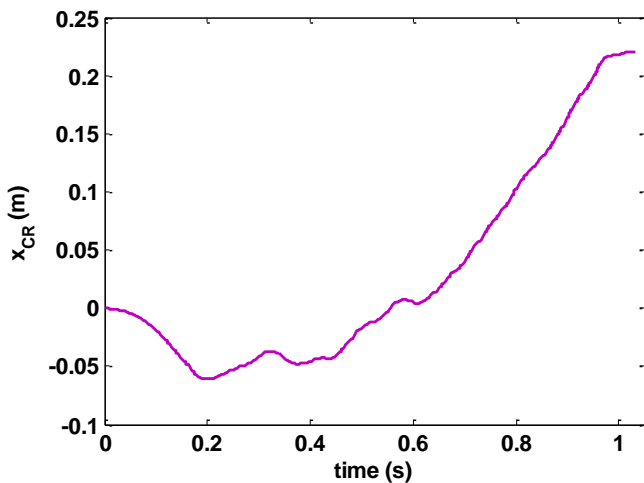


Fig. 17: Cradle vertical displacement

Since only one sensor was used it was not possible to get the angular motion of the elevation parts. Then the results could be used for the estimation of the linear vibration of the system after the end of firing. The last 100 samples were inserted for the spectrum density calculation of the cradle linear vibration. The result of the calculation is shown in Fig. 18.

These results could be used for stiffness determination of the model in Fig. 1, and for comparison of the frequencies belonging to turret vibration. Frequencies around 18 Hz belonged to linear vibration of the turret and frequencies higher than 43 Hz belonged to the elevating parts (cradle).

C. Turret vibration

The cradle motions previously considered were absolute motions; hence the motions were defined with respect to base space, i.e. to the Earth. The turret motion was measured with respect to the hull. Identically, for the linear turret disappearing vibration we can proceed in the same way as in the previous linear cradle vibration.

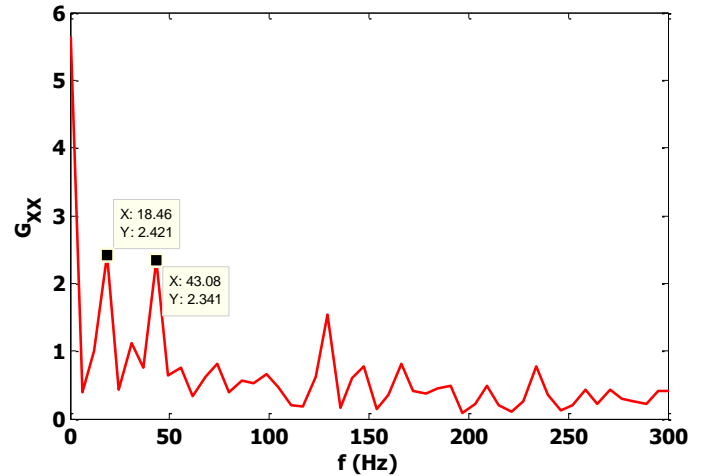


Fig. 18: Cradle disappearing vibration

Although the graphs of turret linear displacement are different in Fig. 5, Fig. 6, their significant similarity is clear from their spectrums. Figures 19 and 20 are the evidence. The frequency of 7.6 Hz is the rate of firing, and 22.7 Hz is most likely the natural frequency of turret angular vibration, as it will be shown further in Fig. 25. An important result is that we can determine the angular stiffness of the turret elastic bearing on the hull.

When the turret mass moment of inertia is known, with respect to the transverse axis passing through the gravity center I_V , the turret angular stiffness is given as

$$k_{y_v} = I_V (2\pi f_{y_v})^2. \quad (11)$$

The linear stiffness of the turret elastic bearing on the hull in the vertical direction is defined in a similar way by the formula

$$k_{y_v} = m_v (2\pi f_{y_v})^2. \quad (12)$$

The individual stiffness in the dynamic model can be set according to the given DOF. In Fig. 1 the whole linear stiffness in the vertical direction is

$$k_{y_v} = k_3 + k_4. \quad (13)$$

for example.

In Fig. 21 there is the disappearing turret linear vibration, and the significant frequencies are near the frequencies belonging to the cradle. Fig. 4 and Fig. 5 show that both signals are time postponed due to time differences in recording

of barrel recoil x_{z_1} and x_{z_2} , y_{VP} and y_{VZ} . It is necessary to put them into the same time relation. The correlation theory is one of the best procedures how to do that. The maximum value of the $R_{x_{z_1}, x_{z_2}}$ normalized cross-correlation function between x_{z_1} , and x_{z_2} signals, stored in both recorders, indicates time lags between the signals, see [7], [28]

$$\tau_{\text{delay}} = \arg \max (R_{x_{z_1}, x_{z_2}}). \quad (14)$$

After insertion into (14), the time delay is 0.112s and it corresponds to 69 postponed samples, see Fig. 22.

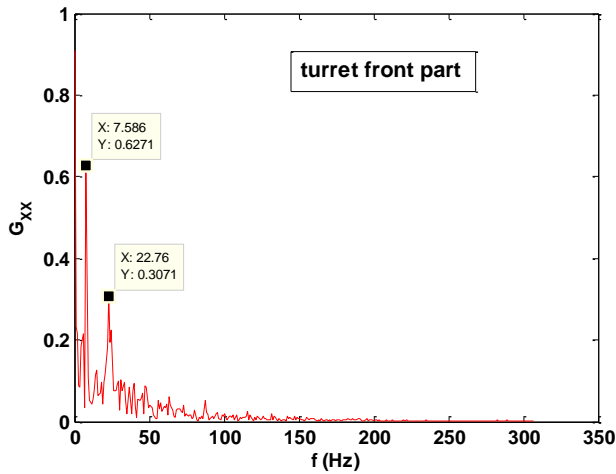


Fig. 19: Turret spectrum of y_{vp}

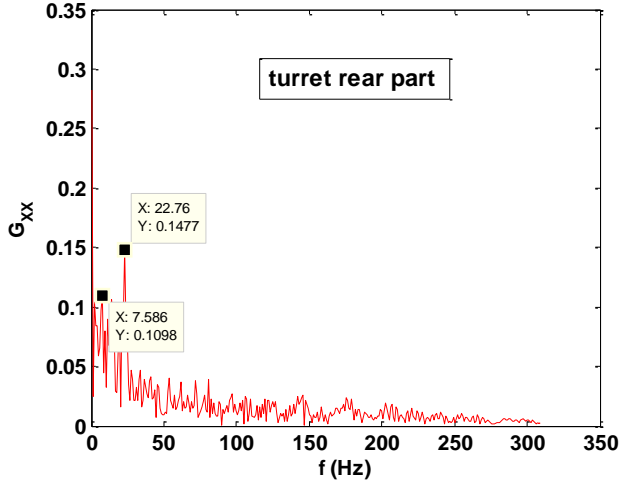


Fig. 20: Turret spectrum of y_{vz}

Then the angular displacement of the turret with respect to the hull can be determined using the simple relation

$$\gamma_V = \frac{y_{VP} - y_{VZ}}{l_s}, \quad (15)$$

where l_s is known distance between both turret sensors.

The time course of the angular turret vibration with respect to the hull is shown in Fig. 23.

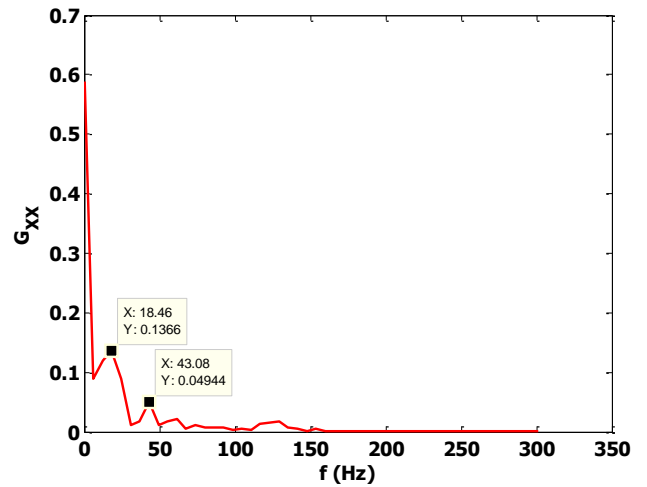


Fig. 21: Disappearing linear turret vibration

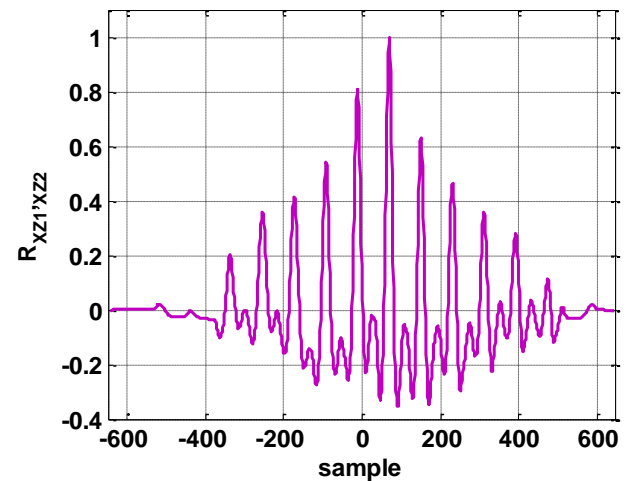


Fig. 22: Cross-correlation function

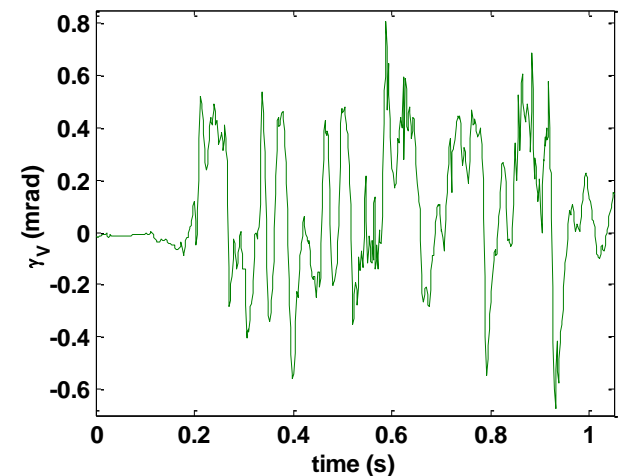


Fig. 23: Angular turret vibration

A better interpretation of turret motion is given by autocorrelation function and the spectral density of vibrations. Figures 24 and 25 prove it. In the autocorrelation function, see Fig. 24, there are distinct peaks belonging to individual shots. It is also shown in Fig. 25, where the basic firing frequency is

7.5 Hz as was explained before. The frequency 22.7 Hz is likely the natural frequency of turret angular vibration.

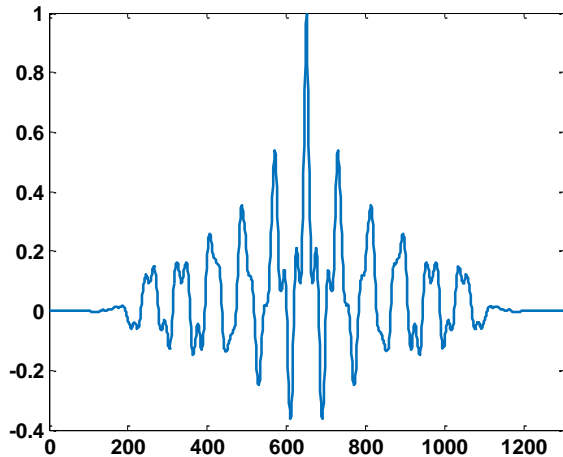


Fig. 24: Autocorrelation function of turret angular vibration

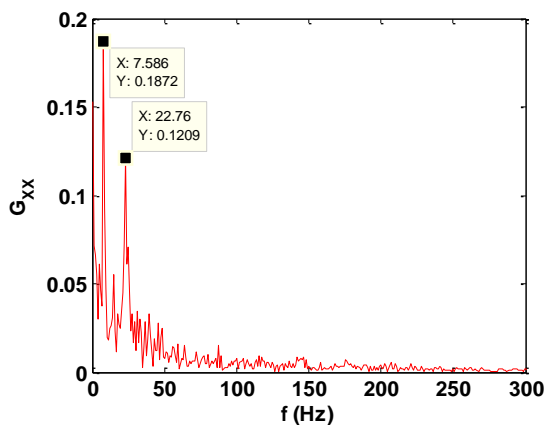


Fig. 25: Turret angular vibration spectrum density

Fig. 25 clearly shows that the rate of fire is lower than natural angular frequency of the turret since the turret motion is able to follow the exciting force. It demonstrates the frequency 22.76 Hz in Fig. 25. The maximal values of angular displacement achieved about 1 mrad. The time course affected the clearances in the turret seating, the elevating parts, and the other parts of the weapon as well. All these clearances were not possible to express because their sizes were not known, and they changed in the course of use.

IV. CONCLUSION

The technical experiments described in this paper are the ground of both the theory and the other investigated dynamics problems of automatic weapon mounts. see [1], [3], [13], [20], [24], and [29]. During preliminary design and testing of weapon systems with automatic weapons we have to be careful to tune the main parts according to Fig. 26. The spectrums of the main parts of the weapon system have to be placed among windows of the force spectrums F_L . Otherwise resonance of the hull, the turret, and the elevating parts (including the cradle, the elevating and traversing gears) can occur. This is the reason why most weapon parts have

additional masses connected with the oscillating parts in order to prevent these undesirable movements.

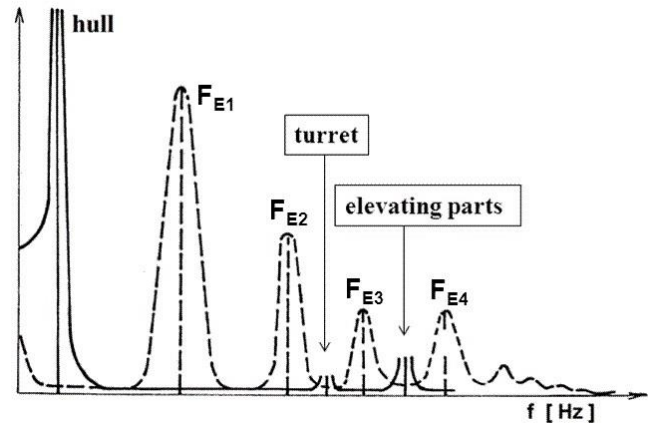


Fig. 26: Spectral density of exciting forces and main parts of weapon systems

REFERENCES

- [1] V. Cech, *Recoil systems I* (Book style). Military academy in Brno. (Czech Republic), 1991, p. 190.
- [2] J. Balla, "Combat vehicle vibrations during fire in burst (Published Conference Proceedings style)", in *The Proceedings of The NAUN/IEEEAM Conferences Mathematical Models For Engineering Science (MMES '10)*. Puerto de la Cruz, Tenerife (Spain), December 2010.
- [3] J. Balla, "Dynamics of Mounted Automatic Cannon on Track Vehicle (Periodical style)", *International Journal of Mathematical Models and Methods in Applied Sciences*. NAUN press, vol. 5, Issue 2, 2011, pp. 423-432. ISSN 1998-0140.
- [4] J. T. Hayes, *Elements of Ordnance. A Textbook for Use of Cadets of the United States Military Academy* (Book style). New York. John Wiley & Sons, Inc. London: Chapman & Hall, Limited, 715 p.
- [5] H. Peter, *Mechanical Engineering. PRINCIPLES OF ARMAMENT DESIGN* (Book style). Trafford Publishing. Suite 6E. 2333 Government St. Victoria. B.C. V8T 4P4, CANADA.
- [6] (Handbook style) *Next View 4.3 professional software documentation*. Maisach (Germany), BMC Messsysteme GmbH, 2009.
- [7] R. Vitek, "Influence of the small arm barrel bore length on the angle of jump dispersion (Published Conference Proceedings style)", in *Proceedings of the 7th WSEAS International Conference on System Science and Simulation in Engineering*, Venice (Italy), November 21 – 23, 2008.
- [8] M. Dub, R. Jalovecky, "DC Motor Experimental Parameter Identification using the Nelder-Mead Simplex Method (Published Conference Proceedings style)". *Proceedings of EPE-PEMC 2010 - 14th International Power Electronics and Motion Control Conference*. Skopje, Republic of Macedonia: Ss Cyril and Methodius University, 2010, p. 9-11. ISBN 978-1-4244-7854-5.
- [9] (Handbook style) *Vibration and Shock Handbook*. Edited by Clarence W. de Silva. CRC Press. Taylor & Francis Group. ISBN 0-8493-1580-8.
- [10] D. F. Allsop, J. Balla, V. Cech, L. Popelinsky, S. Prochazka, J. Rosicky. *Brassey's Essential Guide to MILITARY SMALL ARMS*. (Book style). London, Washington. Brassey's, 1997.
- [11] J. Balla, R. Mach, "Kinematics and dynamics of Gatling weapons (Periodical style)", *Advances in Military Technology*, 2007, vol. 2, no. 2, p. 121-133. ISSN 1802-2308.
- [12] J. Balla, R. Mach, "Main resistances to motion in Gatling weapons (Periodical style)", *Advances in Military Technology*, 2007, vol. 2, no. 1, p. 23-34. ISSN 1802-2308.
- [13] J. Balla, M. Havlicek, L. Jedlicka, Z. Krist, F. Racek, "Firing stability of mounted small arms (Periodical style)", *International Journal of Mathematical Models and Methods in Applied Sciences*. NAUN press, vol. 5, Issue 3, 2011, pp. 412-422. ISSN 1998-0140.
- [14] E. Celens, G. Plovie, "Recoil of small arms (Unpublished work style)", unpublished. Royal Military Academy, Department of Armament and Ballistics. Brussels (Belgium), 1999.

- [15] L. Jedlicka, S. Beer, M. Videnka, "Modelling of pressure gradient in the space behind the projectile (Published Conference Proceedings style)", in *Proceedings of the 7th WSEAS International Conference on System Science and Simulation in Engineering*, Venice (Italy), November 21 – 23, 2008.
- [16] D. Dyckmans, E-book in Ballistics. Theory and software [Online]. Royal Military Academy Brussels, Department of Weapon Systems & Ballistics. (Belgium). Available: <http://e-ballistics.com>.
- [17] *Textbook of Ballistics and Gunnery. Volume One. Part I - Basic theory. Part II - Applications and Design* (Book style), London. Her Majesty's Stationary office, 1987.
- [18] *Handbook on Weaponry*. Rheinmetall GmbH, Düsseldorf. Second English Edition, 1982.
- [19] J. Balla, M. Havlicek, L. Jedlicka, Z. Krist, F. Racek, "Dynamics of automatic weapon mounted on the tripod (Published Conference Proceedings style)" in *The 12th WSEAS International Conference on Mathematical and Computational Methods in Science and Engineering (MACMESE '10)*. Algarve (Portugal), November 2010, pp. 122-127.
- [20] J. Balla, L. Popelinsky, Z. Krist "Theory of High Rate of Fire Automatic Weapon with Together Bound Barrels and Breeches (Periodical style)", *WSEAS Transactions on applied and theoretical mechanics*, 2010, Vol. 5, No. 1, pp. 71-80. ISSN: 1991-8747.
- [21] J. Balla, J. Horvath, "Gas drive of machine gun (Published Conference Proceedings style)", *The Proceedings of The ICMT'11 - International Conference on Military Technologies 2011*. Brno, Czech Republic, University of Defence, 2011, p. 1645-1654. ISBN 978-80-7231-787-5.
- [22] M. Fiser, L. Popelinsky, *Small Arms* (Book style). Brno: University of Defence, 2007.
- [23] *Engineering Design Handbook. Guns Series. Automatic Weapons*. Headquarters, U.S. Army Materiel Command, February, 1970.
- [24] J. Balla, Z. Krist, C. I. Le, "Experimental investigation of weapon system mounted on track vehicle (Published Conference Proceedings style)". *The Proceedings of the 5th International Conference on Theoretical and Applied Mechanics (TAM'14)*. Lisbon, Portugal: WSEAS Press, 2014, p. 166-172. ISSN 2227-4588. ISBN 978-960-474-396-4.
- [25] D. Datuashvili, C. Mert, A. Milnikov, "A New Approach to Detecting Deterministic Periodic Components in Noise (Published Conference Proceedings style)". *The Proceedings of Latest Trends in Circuits, Systems, Signal Processing and Automatic Control*, Salerno, Italy: WSEAS Press, 2014, p. 70-75. ISBN: 978-960-474-374-2.
- [26] A. Milnikov, Pseudospectral "Structure of the Singular Vectors of Nonstationary Time Series (Published Conference Proceedings style)". *The Proceedings of Latest Trends in Circuits, Systems, Signal Processing and Automatic Control*, Salerno, Italy: WSEAS Press, 2014, p. 97-102. ISBN: 978-960-474-374-2.
- [27] R. Ogorkiewitz, *Technology of Tanks I, II* (Book style). London: UK Biddles Limited Guilford and King's Lynn, 1991.
- [28] K. Zaplatilek, J. Leuchter, "Optimal Polynomial Approximation of Photovoltaic Panel Characteristics Using a Stochastic Approach (Periodical style)", *Advances in Military Technology*, 2013, vol. 8, no. 2, p. 43-51, ISSN 1802-2308.
- [29] G. Chinn, *The Machine Gun. Volume V* (Book style), Edwards Brothers Publishing Co., Ann Arbor Michigan, 1987.

Jiri Balla born in Poprad (Czechoslovakia), 6th June 1954. MSc degree in mechanical engineering at Military academy in Brno 1978. PhD degree in field weapons and protection against them at Military academy in Brno 1986. Assoc Prof of Military academy in Brno 1998 in field military technology, weapons and ammunition. Professor of Defense University in Brno 2006 in same field as Assoc Prof. Current the author's major field of study is dynamics of weapon barrel systems. He worked in military units as ordnance officer. After PhD studies he was a teacher as lecturer and associate professor. He was visiting fellow at Royal Military College and Science (RMCS) in Shrivenham (UK) 1996, 1997, 1998. Currently he is a professor at University of Defense in Brno at Weapons and ammunition department, and a professor at Alexander Dubček University of Trenčín, Študentská 2, 911 50 Trenčín, Slovakia.

The main books:

1. Allsop, D. F., Balla, J., Cech, V., Popelinsky, L., Prochazka, S., Rosicky, J. *Brassey's Essential Guide to MILITARY SMALL ARMS*. London, Washington. Brassey's, 1997.
2. Balla, J. *Loading of guns*. Textbook in Czech, Brno, 1998.
3. Popelinsky, L., Balla, J. *Weapons of high rate of fire*. Book in Czech. Prague, D-Consult publishers, 2005.

Prof. Balla is member of Czech Association of Mechanical Engineers (CzAME).

Zbynek Krist born in Kyjov (Czech Republic), 6th December 1974. MSc degree in weapons and munition at Military academy in Brno 2000, PhD degree in the field of weapons and munition at University of Defence 2008. Currently he works as a lecturer at University of Defence in Brno at Department of Weapons and ammunition. His main areas of interest are small arms, weapons mounting, and gunnery.

Cong Ich Le born in Hanoi (Vietnam), 12th March 1979. MSc degree in weapons and munition at Military academy in Hanoi 2003, Magister degree in the field of weapons and munition at Military academy in Hanoi 2008. Currently he works as a PhD student at University of Defence in Brno at Department of Weapons and ammunition. His main areas of interest are small arms, and weapons mounting.